Study of Quantum Dynamics in the Transition from Classical Stability to Chaos

J. C. Robinson, C. Bharucha, F. L. Moore, R. Jahnke, G. A. Georgakis, Q. Niu, and M. G. Raizen
Department of Physics, The University of Texas at Austin, Austin, Texas 78712-1081

Bala Sundaram
Department of Physics and Center for Theoretical Physics, Texas A & M University, College Station, Texas 77843-4242
(Received 1 December 1994)

We report an experimental and theoretical study of momentum transfer from a modulated standing wave of light to a sample of ultracold atoms. This system is a quantum realization of the periodically driven rotor where the underlying classical phase space goes from stable to chaotic as a control parameter is varied. Our experimental results are in good absolute agreement with a quantum Floquet analysis and with a quantum simulation. We relate the quantum evolution to the underlying classical dynamics in this mixed phase space regime.

PACS numbers: 05.45.+b, 32.80.Pj, 42.50.Vk, 72.15.Rn

The transition to chaos in classical Hamiltonian systems has been the topic of great interest in recent years. A parallel effort has been the study of systems which undergo a transition from a regime which can be described classically to one that is manifestly quantum mechanical. These two seemingly disjoint areas come together in quantum systems for which the underlying classical dynamics undergo a transition from stability to chaos as a control parameter is varied. While this problem has been the focus of much theoretical work, experimental progress has been more limited [1], and many key predictions have yet to be verified.

In this Letter we report an experimental and theoretical study of a quantum system for which the underlying classical phase space is composed of islands of stability and regions of chaos. By varying a control parameter the phase space goes from global stability to chaos and is mixed in between. Our system consists of a dilute sample of ultracold atoms in a modulated standing wave of near-resonant light. Momentum transferred to the atoms is measured as a function of the modulation amplitude, which is one of the main control parameters. In previous work we measured momentum transfer in a classically chaotic regime and observed dynamical localization [2]. The focus of this work is to relate the quantum evolution of this system to the underlying classical dynamics. We compare our experiment with a quantum simulation and with a quantum Floquet analysis and find good absolute agreement [3].

Consider the problem of a two level atom (transition frequency ω_0) interacting with a standing wave of near-resonant light (frequency ω_L), where the position of the standing wave nodes are modulated at an angular frequency ω_m and with an amplitude ΔL. For sufficiently large detuning $\delta_L = \omega_0 - \omega_L$ (relative to the natural linewidth), the excited state amplitude can be adiabatically eliminated, leading to a Hamiltonian for the ground state [4] $H = p_x^2/2M - (\hbar\Omega_{\text{eff}}/8)\cos[2k_L(x - \Delta L \sin\omega_m t)]$, where the effective Rabi frequency is $\Omega_{\text{eff}} = \Omega^2/\delta_L$ and k_L is the wave number (Ω is the resonant Rabi frequency, proportional to the square root of the standing wave intensity). The Schrödinger equation describes the evolution of the center-of-mass wave packet of the atom in an effective potential. Switching to scaled dimensionless variables $\tau = \omega_m t$, $\phi = 2k_L x$, $p = (2k_L/M\omega_m)p_x$, and $\mathcal{H} = (4k_L^2/M\omega_m^2)H$, we obtain $\mathcal{H} = p^2/2 - k\cos(\phi - \lambda\sin\tau)$, which is the dimensionless Hamiltonian for a periodically driven rotor. The amplitude is $k = \omega_r\Omega_{\text{eff}}/\omega_m^2$, where $\omega_r = \hbar k_L^2/2M$ is the recoil frequency and $\lambda = 2k_L\Delta L$ is the modulation amplitude.

To study the classical dynamics of this time-dependent problem it is instructive to look at the Fourier expansion of the interaction Hamiltonian $k\cos(\phi - \lambda\sin\tau) = \sum_{m=-\infty}^{\infty} kJ_m(\lambda)\cos(\phi - m\tau)$, where $J_m(\lambda)$ are ordinary Bessel functions of integer order. The stationary phase condition results in resonances at $p = \dot{\phi} = m$ which have approximate widths $4\sqrt{k|J_m(\lambda)|}$ in momentum. Resonance overlap provides a simple estimate of the range of λ for which the classical particle diffuses in momentum. This is most useful in the large λ limit, where odd and even Fourier weights are added separately leading to a two-kick map description of the dynamics. We concentrate here on values of λ, where the modulations in diffusion due to the oscillatory character of the Bessel functions have to be considered, limiting the accuracy of a map description. Instead we numerically integrate Hamilton's equations and use two different sets of initial conditions. The first is a grid in (ϕ, p) space from which phase portraits are constructed. The second mimics the experimental conditions, where the p are Gaussian distributed while the ϕ are uniformly distributed in the interval $[0, 2\pi]$.

The variation of the classical rms momentum width as a function of λ is shown in Fig. 1 (dash-dotted line). Momentum transfer in this problem occurs primarily when the velocities of the atom and the standing wave are matched. Such resonant kicks (RK) occur twice each

0031-9007/95/74(20)/3963(4)$06.00

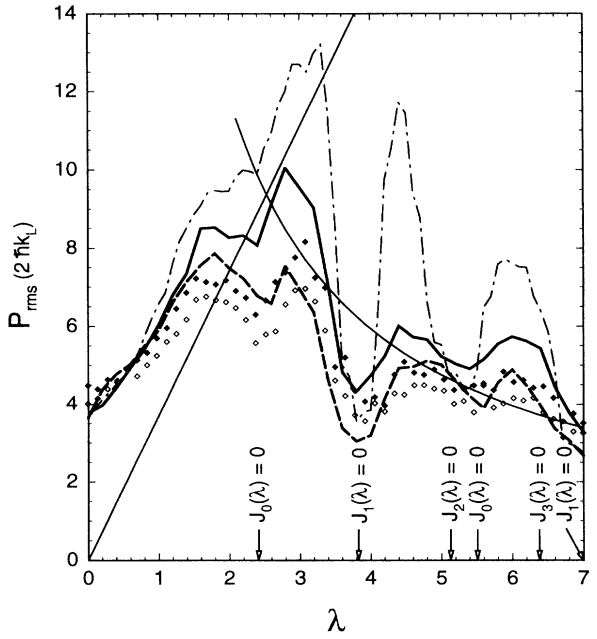

FIG. 1. The rms momentum width as a function of the modulation amplitude λ. Experimental data is denoted by diamonds and have a 10% uncertainty in momentum associated with them. The empty diamonds are for an interaction time of 10 μs and the solid diamonds are for 20 μs; classical simulation for 20 μs (dash-dotted line); quantum Schrödinger for 20 μs (heavy dashed line); quantum Floquet in the long-time limit (heavy solid line). The light solid lines denote the RK boundary and the curve proportional to λ^{-1} predicted in Ref. [4]. $k_{\rm rms} = 0.37$, $k = 0.16$, $\omega_m/2\pi = 1.3$ MHz. A 5% systematic uncertainty in k is due to laser power calibration.

period, although they are not equally spaced in time. When the atomic velocity exceeds the maximum velocity of the standing wave the RK turn off. This leads to an RK boundary that scales linearly with λ (light solid line). At small λ, the distribution quickly saturates near the RK boundary. As λ is increased oscillations occur with the dips corresponding to zeros of the Bessel functions. The overall amplitude of the oscillations decreases as λ is increased, due to the reduction of the size of each RK. The classical simulation for different times shows that the peaks grow until the RK boundary, while the dips grow at a much slower rate. This difference in rates is explained by the phase portraits shown in Fig. 2 (top panel). The peaks are predominantly chaotic while the dips are nearly integrable. The classical line shapes in Fig. 2 (middle panel) clearly show these features as well as the effect of the RK boundary. Initial conditions contained within an island remain trapped, while those in the chaotic domain diffuse up to the boundary, leading to "boxlike" distributions. A clear example of the stability at the dips is at $\lambda = 3.8$, where J_1 has its first zero. The final momentum spread in this case is governed by the surviving island due to J_0 which has a substantial overlap with the initial distribution.

We now turn to the experimental study of momentum transfer from a modulated standing wave to a collection of ultracold atoms. A schematic outline of the experiment is given below (a more detailed description is in Ref. [2]). Sodium atoms are first trapped and laser cooled in a magneto-optic cell trap (MOT) [5]. This prepares the initial conditions for the experiment which are Gaussian distributed in momentum and position. Note that the spread in position is uniform on the scale of the nodes of the standing wave. The spread in position on the larger scale leads to a 10% variation of k across the atomic sample. After the cooling and trapping stage, the MOT is turned off, and the modulated standing wave is turned on for a controlled time (typically, 10–20 μs), during which growth in momentum occurs along the direction of the modulated standing wave. The probability of a spontaneous emission event during a modulation period is below 1.0% in this work. After the standing wave is turned off, the atoms undergo free expansion in the dark for a controlled time (typically, several ms). The momentum distribution is reflected in the positions of the atoms after the free expansion time. This position is "frozen" in with optical molasses [5], and the resulting atomic fluorescence is imaged on a charge coupled device camera. The initial size of the MOT is deconvolved, and the measurement of position is converted into a momentum spread using the free expansion time. We also use this technique to measure the initial momentum distribution by repeating the measurement cycle with the modulated standing wave off. Our initial momentum spread is Gaussian distributed with $\sigma = 4.6\hbar k_L$, and the resolution of this measurement can be subrecoil. We have measured the momentum distributions for λ with values $0 \rightarrow 7$ in order to cover the full range of mixed phase space dynamics. The measured rms momenta vs λ are shown in Fig. 1 (diamonds). The empty diamonds are for an interaction time of 10 μs and the solid diamonds are for 20 μs, showing that these results are close to saturation for the range of λ that is shown. Note that for small values of λ there is good agreement with the classical prediction. At $\lambda = 0$ the system is integrable and momentum is trivially localized. As λ is increased the phase space becomes chaotic, but growth is limited by the RK boundary. Our measured momentum distributions (in Fig. 2, bottom panel) are characteristically boxlike in this regime ($\lambda = 1.5$). As λ is increased beyond a critical value there are oscillations in localization with an rms spread that deviates substantially from the classical prediction at the peaks. For those values of λ the classical phase space is predominately chaotic, and exponentially localized distributions are observed because the quantum break time occurs before the RK boundary is reached. This is shown in Fig. 2 for $\lambda = 3.0$. At the dips in oscillation, as in the case $\lambda = 3.8$, the classical phase space becomes nearly integrable and the measured momentum is close to the classical prediction. In the intermediate regime the phase space is mixed and the momentum distributions exhibit features which can be clearly identified with the

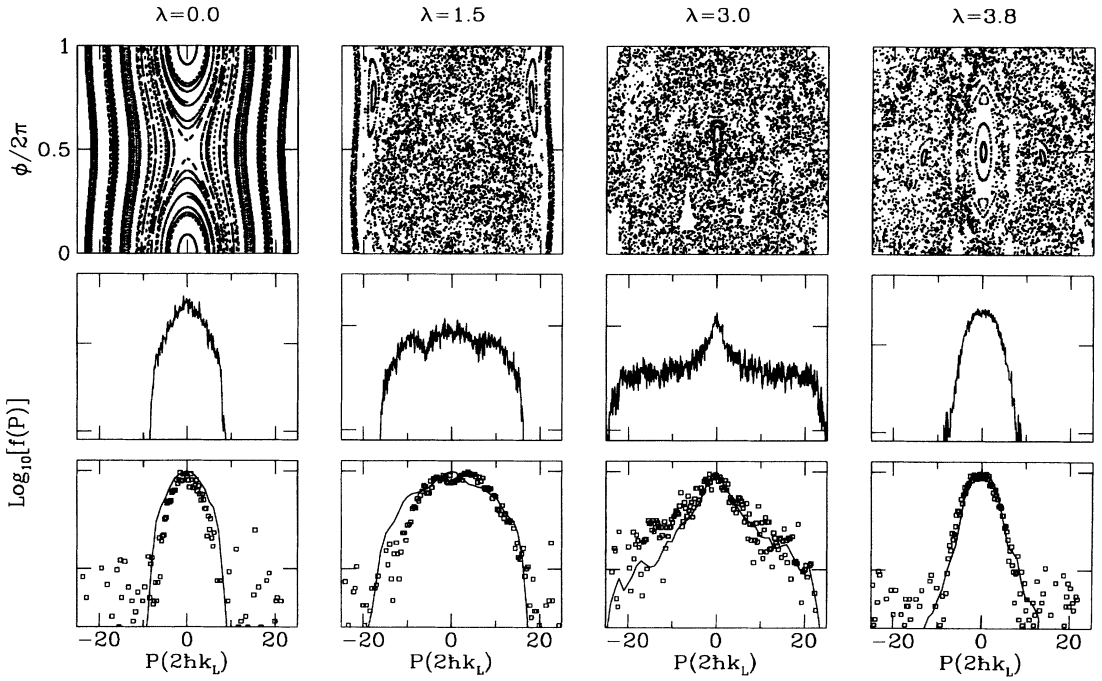

FIG. 2. Phase portraits (upper panel), classical momentum distributions (middle panel), and experimentally measured momentum distributions with Floquet theory (bottom panel, theory marked by lines) for runs with parameters similar to those in Fig. 1. Note that the vertical scales for the distributions are logarithmic and are marked in decades.

underlying classical phase space. In Fig. 3(a), there is a boxlike distribution with a Gaussian-like peak in the center. This corresponds to part of the initial conditions that is trapped in an island of stability and part that diffuses out to uniformly fill the chaotic phase space within the RK boundary. In Fig. 3(b) λ is larger and the RK boundary is farther away. Now the part of the initial conditions contained in the chaotic domain becomes exponentially localized, while the island structure leads to a similar effect as in Fig. 3(a). Both figures illustrate the unique potential of this experiment to study issues of structure and transport in a mixed phase space.

To compare with experiment we have performed a space-time integration of the Schrödinger equation using a standard two-sweep method [6]. A single particle wave packet initial condition mimics the ensemble of independent atoms in the experiment for which the width in p is Gaussian while the spatial width in ϕ is limited by the spread of the MOT. In our system of scaled units these widths are related by the commutator $[\phi, p] = i\hbar$, where $\hbar = 8\omega_r/\omega_m$. Our choice was a "squeezed" wave packet given by $\psi(\phi) = (2\pi\mu)^{-1/4}\exp[i(A(\phi - \phi_0)^2 + p_0(\phi - \phi_0)/\hbar)]$, where (ϕ_0, p_0) are the centroid (mean) values and the variances [with respect to (ϕ_0, p_0)] are $\langle\Delta\phi^2\rangle = \mu$, $\langle\Delta\phi\Delta p + \Delta p\Delta\phi\rangle = \alpha\hbar$, and $4\mu\langle\Delta p^2\rangle = \hbar^2(1 + \alpha^2)$, from which we get that $A = (i + \alpha)/4\mu$. The widths in p and ϕ are independently determined by adjusting α to maintain the minimum uncertainty condition. This initial condition is evolved under the Schrödinger equation for fixed interaction time and $p_{\rm rms}$ is computed. The results are shown by the heavy dashed line in Fig. 1 and are in close absolute agreement with experiment with no adjustable parameters.

To gain further insight into this problem, we have also done a quantum Floquet analysis. The eigenstates of our Hamiltonian are most naturally represented using a 2D Floquet state basis, $\{\psi(\phi, \tau) = e^{iq\phi}e^{-i\epsilon\tau}u(\phi, \tau)\}$. Here $u(\phi, \tau)$ reflects the periodic structure of the Hamiltonian;

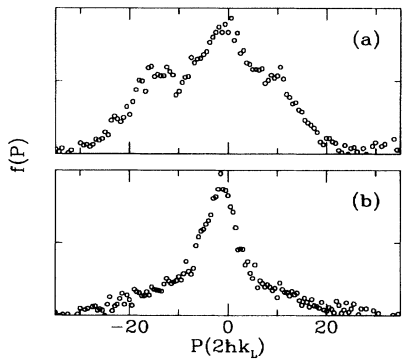

FIG. 3. Experimental momentum distributions for two cases in a mixed phase space regime. In (a) λ is below the crossover, and growth is limited at the RK boundary. In (b) λ is above the crossover and initial conditions in the chaotic regime are exponentially localized. In both cases initial conditions in islands of stability remain trapped. Note that the vertical scale here is linear.

that is $u(\phi + 2\pi, \tau) = u(\phi, \tau + 2\pi) = u(\phi, \tau)$, where q is the quasimomentum and ϵ is the quasienergy [7]. Expanding $u(\phi, \tau)$ in a Fourier series, in both the space and time variables, allows us to write the quasienergy-momentum states in the form $\psi_\epsilon(\phi, \tau) = \sum_{mn} \psi^\epsilon_{mn} e^{i(q+n)\phi} e^{-i(\epsilon+m)\tau}$. The Schrödinger equation in this representation is then

$$\epsilon \psi^\epsilon_{mn} = [-m + (n + q)^2/2]\psi^\epsilon_{mn} - \frac{k}{2\hbar} \sum_{l=-\infty}^{\infty} J_l(\lambda)(\psi^\epsilon_{m-l,n-1} + \psi^\epsilon_{m+l,n+1}). \quad (1)$$

For each q, the set of quasienergies and the corresponding quasienergy-momentum states are obtained by numerically solving Eq. (1). To make contact with the experiment, we use appropriate initial conditions and find the Floquet basis representation. The quantities $(q + n)$ and $(\epsilon + m)$ are identified, respectively, with momentum and energy. The solution is then averaged in time to give the long-time results. To simplify the Floquet analysis, the small spread in k proportional to laser intensity variations across the ensemble of atoms is approximated by the use of an rms k. The rms momentum spread from the Floquet analysis is shown in Fig. 1 (heavy solid line) and the line shapes are given in Fig. 2 (bottom panel). For both cases there is good agreement with experiment over the range of λ.

The Schrödinger equation has the form of a two-dimensional tight-binding "eigenenergy" (ϵ) equation with "site energy" $-m + \hbar(q + n)^2/2$ and hopping terms of energy $k/2\hbar$. For a given state, the site energy cannot differ from the eigenenergy by much more than the "hopping energy." Since we can choose both ϵ and q to be within the interval [-1/2, 1/2], each wave function is confined to a parabolic strip centered about the curve $\epsilon + m = \hbar(q + n)^2/2$ as shown in Fig. 4. The points along the parabola denote the expectation values of $\epsilon + m$ and $q + n$ for each Floquet state. The error bars denote the corresponding rms widths. With the locus of states confined to a region about the parabola the problem is essentially reduced to one dimension. Furthermore, along this quasi-1D array of points there is no apparent order, which is reminiscent of the disordered lattice underpinning the theory of Anderson localization [8]. Beyond this connection to condensed matter physics, our system is directly analogous to the current-driven Josephson junction [9], and heating of a Bloch electron in an ac field [10], and can serve as a testing ground without the complications of impurities, multiparticle interactions, and thermal effects. The latter can be introduced in a controlled manner which will be the topic of future work.

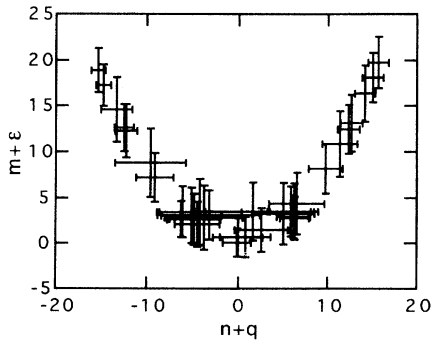

FIG. 4. Theoretically calculated positions and rms widths of the Floquet states in the $(\epsilon + m, q + n)$ space for $\lambda = 5.0$, $k = 0.37$, and $\hbar = 0.16$.

Looking towards future studies of quantum dynamics in a mixed classical phase space it is clear that initial conditions that are also confined in ϕ could open new areas of research. For example, if the atoms are initially prepared within an island of stability, it may be possible to directly observe dynamical quantum tunneling. Control of initial conditions may also enable a direct study of quantum scars [11,12].

We thank Wolfgang Schleich and co-workers for sending us a preprint of their theoretical paper in which they independently obtain similar results [13]. The work of M. G. R. is supported by the ONR Young Investigator Program, the R. A. Welch Foundation, and the NSF Young Investigator Program. The work of Q. N. is supported by the R. A. Welch Foundation, and the work of B. S. is supported by the NSF.

[1] See contributions in *Irregular Atomic Systems and Quantum Chaos,* edited by J. C. Gay (Gordon & Breach, New York, 1992).
[2] F. L. Moore, J. C. Robinson, C. Bharucha, P. E. Williams, and M. G. Raizen, Phys. Rev. Lett. **73**, 2974 (1994).
[3] We reported this work at the 4th Drexel Symposium on Quantum Nonintegrability, Sept. 8–11, 1994.
[4] R. Graham, M. Schlautmann, and P. Zoller, Phys. Rev. A **45**, R19 (1992).
[5] Laser cooling and trapping is reviewed by Steven Chu in Science **253**, 861 (1991).
[6] S. E. Koonin and D. C. Meredith, *Computational Physics* (Addison Wesley, Menlo Park, 1990).
[7] Ya. B. Zeldovich, JETP **24**, 5 (1967).
[8] D. J. Thouless, Phys. Rep. **13**, 93 (1974); Shmuel Fishman, D. R. Grempel, and R. E. Prange, Phys. Rev. Lett. **49**, 8 (1982).
[9] R. Graham, M. Schlautmann, and D. L. Shepelyansky, Phys. Rev. Lett. **67**, 2 (1991).
[10] Doron Iliescu, Shmuel Fishman, and Eshel Ben-Jacob, Phys. Rev. B **46**, 14 675 (1992).
[11] E. J. Heller and S. Tomsovic, Phys. Today **46**, 38 (1993).
[12] Note that the oscillating sign of J_0 leads to the exchange of stability between the primary hyperbolic and elliptic fixed points. The effect is clearly visible on contrasting the phase portraits for $\lambda = 0$ and $\lambda = 3.0$, which is beyond the first zero of J_0 at $\lambda = 2.41$. This is equivalent to changing the sign of the stochasticity parameter in the standard map and may be useful in the context of scarring.
[13] P. J. Bardroff, I. Bialynicki-Birula, D. S. Krähmer, G. Kurizki, E. Mayr, P. Stifter, and W. P. Schleich, preceding Letter, Phys. Rev. Lett **74**, 3959 (1995).